Heat Mass Transfer
DOI 10.1007/s00231-016-1930-2

ORIGINAL

Spray mist cooling heat transfer in glass tempering process

Nedim Sozbir[1] · **S. C. Yao**[2]

Received: 19 March 2015 / Accepted: 4 October 2016

Abstract Energy saving is a very important issue in glass plants, especially in a glass tempering process, where very high velocity air jet impingement is applied during the cooling process of glass tempering. In fact, air compressor energy may be reduced by a spray cooling due to its high heat transfer capabilities. Presently, in this paper, both pure air and water mist spray cooling are investigated in the glass tempering process. The test results indicate that thin and low-cost tempered glass can be made by mist cooling without fracture. It is possible to find the optimal water flux and duration of mist application to achieve a desirable temperature distribution in the glass for deep penetration of the cooling front but without inducing cracking during the tempering. The use of mist cooling could give about 29 % air pressure reduction for 2-mm glass plate and 50 % reduction for both 3- and 4-mm glass plates.

1 Introduction

Generally, many industrial applications require effective and rapid cooling process from high temperatures such as thin plates in the hot rolling steel mill, glass tempering in the auto industry, cooling of electronic devices, and space applications. Spray cooling has been used in some engineering processes [1, 2], such as the metallurgical industries for the cooling of high temperature metals at film boiling. Water mist cooling at film boiling condition can be also used in many other industrial applications because of its high heat transfer rate.

Sprays are made of large drops, in the order of 100 μm or larger, and operated at high mass flux to give high heat transfer rates. However, the heat transfer distribution frequently is not uniform and water utilization efficiency is low. Recently, more and more industrial processes use water mist for cooling. Water mist contains small droplets, on the order of or less than 100 μm, and caries co-flowing air which are entrained or are used for atomization. The mass flux of water mist is low and therefore, the heat transfer rate is not as high as sprays; however, the water mist provides relatively uniform heat transfer and has high water usage efficiency. Furthermore, both water and air flow rates can be adjusted respectively to provide a wide range of heat transfer. Due to these advantages, water mists are used preferably for cooling of thin metal sheets and for tempering of glass at high temperature film boiling conditions.

In the high temperature film boiling regime, the impacting droplets of water mist will contact the surface for a very short period of time; however, the resulting heat transfer is significant. The contact heat transfer mechanisms include the convection in the layer of vapor forming underneath the droplets and transient homogeneous nucleation at the point of droplet-surface contact. In addition to the droplet contact heat transfer, there is radiation from the surface and convection associated with bulk air blowing over the surface. Due to the droplets-to-surface contacts, material properties and roughness also influence the heat transfer [3–5].

Energy efficiency improvement opportunities exist within glass plants to improve energy efficiency while maintaining or enhancing productivity. Improving energy efficiency

✉ Nedim Sozbir
sozbir@sakarya.edu.tr

S. C. Yao
scyao@cmu.edu

[1] Department of Mechanical Engineering, Sakarya University, 54187 Esentepe, Sakarya, Turkey

[2] Department of Mechanical Engineering, Carnegie Mellon University, Pittsburgh, PA 15213, USA

Published online: 21 October 2016

at a glass plant should be approached from several directions. First, a glass plant uses energy for equipment such as motors, pumps, and compressors. A second and equally important area is the proper and efficient operation of the processes. Process optimization and ensuring that the most productive technologies are in place are keys to realizing energy savings in a plant's operation. Finally, throughout a glass plant, there are many processes in operation at the same time. Coordinating their efficiency and operation is necessary to ensure energy savings are realized [6, 7].

Tempered glass has been used as safety sight glass for pressure gauges, safety glasses and automobile windshields, trains, ships, airplanes, lamps, architectural applications and numerous other applications. Comprehensive studies of glass tempering have been reviewed [8–11]. Tempering is a process that entails heating of the material to beyond the annealing temperature and afterwards rapidly quenching it from 650 °C. Consider a heated glass surface that is cooled at the surface at a uniform rate. The temperature distribution will be roughly parabolic and will remain that way as long as the time rate of the surface temperature change remains constant. Suppose the temperature gradient has reached a stable state while the glass is still soft and thus unable to retain the temporary stresses caused by the introduction of this gradient. The glass will not be under stress while the temperature gradient is being established, nor, so long as it is being cooled at a uniform rate, will any stress develop. However, when the glass is eventually cooled to near the ambient temperature over the total thickness, the center will tend to shrink and cause high compression in the surface.

There will be no sharp fragments when the tempered glass is broken. The enhancement of breaking strength is not the only attribute sought in tempered glass. The fragments of the tempered glass should be made less dangerous than the sharp, often dagger-like fragments of non-tempered glass. Large fragments are the consequence of the glass when it is insufficiently tempered. Thus, when the insufficiently tempered glass breaks under a relatively low load, the stress energy in the glass at the moment of the fracture is also low, and correspondingly, little new surface is created in the fracture process. Therefore, the well-tempered glass is not only stronger, allowing more stress energy to be stored in it by greater external loads, but the temper stresses themselves impart to the glass a high content of the stress energy even in the absence of the external loading. Therefore, when the tempered glass is broken, its stress energy is always high enough to reduce the glass into usually harmless small fragments, more or less cubical in shape. In conclusion, controlling the temperature history during the tempering process is very important.

Many researchers have studied transient and steady state combined conduction and radiation in glass [12–16]. Most of researchers have evaluated the transient temperature distribution by considering the combined forced convection and radiation cooling from surfaces. On the other hand, mist cooling has been used extensively in many cooling applications because of the high heat transfer rate. One of the well-known applications is in the steel industry. However, it is still questionable whether the mist cooling technique can be applied to materials of poor thermal conductivity such as glass because the boiling heat transfer is sensitive to the surface conductivity and temperature.

The minimum film boiling heat flux on the material occurs at the Leidenfrost temperature. It is known that mist cooling applied below the Leidenfrost temperature will induce severe and uneven stresses due to the high heat flux of local nucleate boiling, and may cause cracking of such brittle material. The Leidenfrost temperature is generally higher for materials of poor thermal conductivities. The temperature zone of the glass tempering process is between 500 and 700 °C. The lower end of the temperature zone is near the Leidenfrost temperature of the glass. Therefore, glass may be cracked when the water impinges on the glass surface while the surface temperature falls lower than the Leidenfrost temperature during the tempering process. Ohkuba and Nishio [13] investigated a feasibility study of glass tempering using mist cooling. First, transient tests of mist cooling were conducted to investigate the effects of the thermal properties of a cooling surface. Second, tempering tests of soda-lime glass plates of 2.95 and 3.90 mm thicknesses were conducted using mist cooling. The initial temperature of the glass plates was about 690 °C. The plates were cooled only from one side. The test results indicated that thin and low-cost tempered glass plates can be made by mist cooling without fracture. Kormanyos [17] investigated controlled differential forced convection heating for glass tempering processes. A forced convection heater based tempering system capable of heating glass loads 2.13 m by 3.66 m was developed and successfully demonstrated. Performance of the system capable was verified through processing glasses ranging in thickness from 2.3 to 19 mm. The heat transfer generated by the convective flow of the heated working fluid (hot air) can be adjusted by changing the impingement velocity of the fluid, the temperature of the fluid, or both. The controls are independent of each other so a large flow with lower temperature air or small flow with higher temperature air can be set on the heating fluids of the top and bottom of ceramic roller bed. The independence of control allows the heater to be tuned so glasses with a variety of colors or surface treatments can be processed effectively. Monnoyer and Lochegnies [18] studied impinging air jet cooling applied to thermal glass tempering. The static tempering of a square flat glass sample in an industrial unit is modelled to assess the convective heat transfer from the

glass surface to the cooling jets. The flow in the air supply nozzles is first investigated to verify the uniformity of the flow conditions at jet outlets. The numerical simulation of the static temperature measurements by pyrometry. Heat transfer coefficients are calculated for four different jets Reynolds numbers. The heat transfer is low compared to other correlations, because of the relatively large the jet height to jet diameter ratio and of the strong cross flow induced by the large amount of spent air. Lochegnies and Monnoyer [19] developed a model to calculate the residual tempering stresses arising during the thermal tempering of flat glass in a static position in an industrial tempering unit. The model is a 3D finite-element model, based on the computational fluid dynamics (CFD) estimation of the heat transfer distribution on the glass surface, and takes structural and stress relaxations into account. First, the inhomogeneous distribution of the residual stresses for a reference air-impinging velocity value are presented and validated by photoelasticity measurements of the surface compression. For other velocities corresponding to the unit's processing capabilities, the numerical results highlight the relationship between heat transfer and stress in terms of average values and in homogeneities on the glass surface. Makarov and Suvorov [20] developed the dependence of the shape of glass on the tempering regime. Simulation of the algorithm controlling the tempering of automobile glass is performed. It is shown that the quality of the glass produced can be further improved. The effectiveness of using simulation in developing corrective actions in the production of tempered glass is validated. Nielsen et al. [21] developed and validates a 3D model for the simulation of glass tempering. It is assembled from well-known models of temperature dependent viscoelasticity and structural relaxation and predicts both transient and steady-state stresses in complex 3D glass geometries. The theory and implementation of the model is comprehensively given and the model is carefully checked and validated. It is demonstrated that by adjusting a single parameter in the model, experimental results can be replicated accurately even for cooling rates far from normal. Golcü et al. [22] studied auto glass tempering. Heat transfer characteristics of heated glass plates during their cooling with mutually placed circular air jet was investigated experimentally. 4 mm thick glass samples were used in the experiments. Cooling process was performed with 16 mutually placed nozzles. Yazıcı et al. [23] investigated experimental transient cooling characteristics of an industrial glass tempering unit. The effect of dimensionless jet to jet distance and jet to plate distance on the cooling time was studied. Akçay et al. [24] designed a prototype tempering glass unit and studied the effect of heating and cooling temperatures on rapid cooling time and particle number in auto glass tempering process. Yazıcı et al. [25] studied experimental investigation of transient temperature

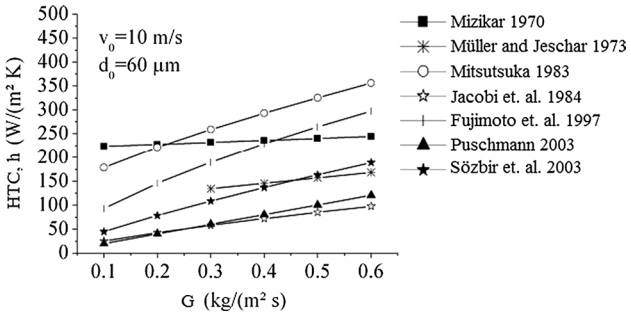

Fig. 1 Calculated heat transfer coefficient (HTC) from various correlations [27]

distribution and heat transfer by jet impingement in glass tempering process. Akçay et al. [26] investigated the effect of different cooling unit configurations and cooling temperatures on glass tempering quality. An auto glass tempering process was conducted in different cooling unit configurations and cooling temperatures, and the changes in the sudden cooling time and the number of broken glass particles of the tempered glass plates were examined.

Many researchers have studied mist heat transfer at this condition and have given empirical, semi empirical or numerical models to describe the cooling process and to calculate the heat transfer coefficient. The calculated heat transfer coefficients are presented in Fig. 1. The heat transfer coefficient mainly depends on the mass flux of the cooling fluid, which is the most important spray parameter of the cooling. Only few of the studies correlate the heat transfer coefficient with the droplet velocity and droplet diameter. The great discrepancies in the different experimental values of the heat transfer coefficient can be seen clearly in Fig. 1. This figure described different trends of the dependence of the heat transfer coefficient on the droplet parameter, diameter and velocity [27].

An attempt was made by Deb and Yao [28], who modeled the spray cooling at film boiling condition by considering droplet impingement heat transfer and air convective heat transfer separately. The overall heat transfer is considered as the summation of these two contributions in addition to radiation cooling. However, no experimental verification was reported in terms of parametric studies of these factors to validate this phenomenon directly. Graham and Ramadhyani [29] and Sozbir et al. [4, 5] investigated water mist cooling for glass tempering and metal plate cooling experimentally. Ideally, for the impaction cooling of dilute water mist at high surface temperature, the heat transfer contribution of air and water could be independent and separable. Cox and Yao [30] performed to evaluate the heat transfer of monodisperse sprays of large droplet diameters, ranging from 3 to 25 mm, on high temperature surfaces experimentally. Yao and Cox [31] developed a method for the general

correlation of heat transfer effectiveness for sprays impacting vertically downward on a high temperature surface. Issa and Yao [32, 33] developed to simulate for atmospheric applications the impingement of water sprays on surfaces heated at temperatures ranging from nucleate to film boiling numerically. Moreira et al. [34] described an experimental methodology devised to study spray cooling with multiple-intermitted sprays as those found in fuel injection system of spark-ignition and diesel engines, or in dermatologic surgery applications. Al-Ahmadi and Yao [35] conducted for the spray cooling of high temperature stainless steel using three different types of industrial sprays experimentally. Full cone, flat hydraulic nozzles and a flat air mist nozzles were used in the experiments. Hernandez et al. [36] developed a model for predicting parameters based on the design and operating characteristics of air mist nozzles and on experimentally determined drop size distributions. Lyons et al. [37] described the experimental heat transfer characteristics of impinging air jets. Panao and Moreira [38] investigated a new approach in the development of heat transfer empirical correlations for intermittent spray impingement, based on simultaneous measurements of the spray droplets characteristics and the surface thermal behavior. Santangelo [39] focused on characterizing the solid cone water- mist spray produced by a typical atomizer at high operative pressure (in the range 60–80 bars). Experimental campaign conducted, mainly employing optical techniques: drop-size and flux distribution, initial velocity and cone angle were investigated to provide a quantitative description of atomization and dispersion. Cheng et al. [40] studied the effects of spray height, nozzle spray angle, inlet pressure and spray incident angle on heat transfer of spray cooling experimentally. Multi-points thermocouples and infrared imaging device were used to measure temperature distribution on heating surface. A Doppler anemometry and a camera were applied to study the spray flow field. The mechanism of heat transfer of spray cooling was concluded on the basis of experimental data and spray characteristics. It is showed that parameters affect heat transfer by way of changing the flow field on the heating surface. Heat transfer performance can be optimized by a smaller spray angle nozzle, which sprays at a smaller spray height and a higher inlet pressure. The effect of incident angle on heat transfer depends on nozzle spray angle and the definition of distance of nozzle to surface. Zhao et al. [41] developed a model to predict the heat and mass transfer in spray cooling. The droplet-film impaction was modeled based on an empirical correlation related with droplet Weber number. The film formation, film motion, bubble growth, and bubble motion were modeled based on dynamics fundamentals. The model was validated by the experimental results provided and a favorable comparison was demonstrated with a deviation below 10 %. The film thickness, film velocity, and non-uniform surface temperature distribution were obtained numerically, and then analyzed. A parameters sensitivity analysis was made to obtain the influence of spray angle, surface heat flux density, and spray flow rate on the surface temperature distribution, respectively. It can be concluded that the heat transfer induced by droplet-film impaction and film surface convection is dominant in spray cooling under conditions that the heated surface is not superheated. However, the effect of boiling bubbles increases rapidly while the heated surface becomes superheated. Sözbir et al. [42] conducted to reveal the heat transfer mechanism of impacting water mist on high temperature surface experimentally. A numerical model was developed to simulate, for atmospheric applications, air and water mist spray cooling of surfaces heated to temperatures ranging from nucleate to film boiling. Yiğit et al. [43] studied experimental measurements and computational modeling for the spray cooling of a steel plate near the Leidenfrost temperature. Panao et al. [44, 45]. studied thermal fluid assessment of multi jet atomization for spray cooling applications and investigated high power thermal management with intermitted multi jet sprays. Lyons et al. [46] studied heat transfer and fluid dynamics in an impinging atomizing air/water mist jet. Bellerová et al. [47] investigated the transient temperatures of a metal testing plate during spray cooling using alumina/water nanofluids. The heat transfer coefficient (HTC) was calculated by an inverse heat-conduction technique using the measured temperatures. The results show a decrease of approximately 20 % of the HTC of spray cooling with the nanoparticle suspension changing from 0 to 16.45 %. The nature and the reason of the HTC deduction were investigated and the HTC correlations with the mass fluxes and nanoparticle fraction were specifically reported. Yan et al. [48] designed and tested an inclined spray chamber with four multiple nozzles to cool a 1 kW 6U electronic test card. The multiple inclined sprays can cover the same heated surface area as that with the multiple normal sprays but halve the volume of the spray chamber. The spray cooling system used R134a as a working fluid in a modified refrigeration cycle. It is observed that increasing mass flow rate and pressure drop across the nozzles improved the heat transfer coefficient with a maximum enhancement of 117 %, and reduced the maximum temperature difference at the heated surface from 13.8 to 8.4 °C in the inclined spray chamber with a heat flux of 5.25 W/cm^2, while the heat transfer coefficient of the normal spray increased with a maximum enhancement of 215 % and the maximum temperature difference decreased from 10.8 to 5.4 °C under similar operating conditions. The multiple inclined sprays could produce a higher heat transfer coefficient but with an increase in non-uniformity of the surface temperature compared with the multiple normal sprays. Ravikumar et al. [49] studied the ultrafast cooling that occurs during high mass flux air-atomized spray

impingement on a hot 6 mm thick stainless steel plate. The nozzle inclination is between 0° and 60°. The average mass flux of water used in the study accounts to 510 kg/m^2 s. The coolants used in the study are pure water and surfactant water of 600 ppm concentration. The initial temperature of the plate has been maintained at 900 °C, which is the temperature of a hot strip on run-out table in steel industry. The transient surface heat flux and temperature histories have been estimated by an inverse heat solver using measured temperature input data. Heat transfer results demonstrates that optimum cooling efficiency (~2.76 MW/m^2, 194 °C/s) for pure water has been achieved at 30° nozzle orientation. The inclined nozzle has not been found beneficial when surfactant water is used as the coolant. Mohapatra [50] studied the applicability of air atomized spray with the salt added water for ultra fast cooling (UFC) of a 6 mm thick AISI-304 hot steel plate. The investigation includes the effect of salt (NaCl and $MgSO_4$) concentration and spray mass flux on the cooling rate. The initial temperature of the steel plate before the commencement of cooling is kept at 900 °C or above, which is usually observed as the "finish rolling temperature" in the hot strip mill of a steel plant. The heat transfer analysis shows that air atomized spray with the $MgSO_4$ salt produces 1.5 times higher cooling rate than atomized spray with the pure water, whereas air atomized spray with NaCl produces only 1.2 times higher cooling rate. In transition boiling regime, the salt deposition occurswhich causes enhancement in heat transfer rate by conduction. Moreover, surface tension is the governing parameter behind the vapour film instability and this length scale increases with increase in surface tension of coolant. Overall, the achieved cooling rates produced by both types of salt added air atomized spray are found to be in the UFC regime. Panao and Delgado [51] studied low flow rate multi jet impingement spray atomizers. Aamir et al. [52] investigated high heat transfer performance of spray cooling on structured surface with an additional measure to increase the safety of an installation against any threat caused by rapid increase in the temperature. The purpose of present experimental study is to explore heat transfer performance of structured surface under different spray conditions and surface temperatures. Two cylindrical stainless steel samples were used, one with pyramid pins structured surface and other with smooth surface. Surface heat flux of 3.60, 3.46, 3.93 and 4.91 MW/m^2 are estimated for sample initial average temperature of 600, 700, 800 and 900 °C, respectively for an inlet pressure of 1.0 MPa. A maximum cooling rate of 507 °C/s was estimated for an inlet pressure of 0.7 MPa at 900 °C for structured surface while for smooth surface maximum cooling rate of 356 °C/s was attained at 1.0 MPa for 700 °C. Structured surface performed better to exchange heat during spray cooling at initial sample temperature of 900 °C with a relative increase in surface heat flux by factor of 1.9, 1.56, 1.66 and 1.74 relative to smooth surface, for inlet pressure of 0.4, 0.7, 1.0 and 1.3 MPa, respectively. For smooth surface, a decreasing trend in estimated heat flux is observed, when initial sample temperature was increased from 600 to 900 °C. Temperature-based function specification method was utilized to estimate surface heat flux and surface temperature. Limited published work is available about the application of structured surface spray cooling techniques for safety of stainless steel structures at very high temperature scenario such as nuclear safety vessel and liquid natural gas storage tanks. Agrawal et al. [53] studied normal impinging round water jet. A stainless steel (SS-316) vertical rod of 12 mm diameter at 800 ± 10 °C initial temperature was cooled. The surface rewetting phenomenon was investigated for a range of jet diameter 2.5–4.8 mm and jet Reynolds number 5000–24,000 using a straight tube type nozzle. The investigation were made from the stagnation point to maximum 40 mm downstream locations, simultaneously for both upside and downside directions. The cooling performance of the vertical rod was evaluated on the basis of rewetting parameters i.e. rewetting temperature, wetting delay, rewetting velocity and the maximum surface heat flux. Two separate Correlations have been proposed for the dimensionless rewetting velocity in terms of rewetting number and the maximum surface heat flux that predicts the experimental data within an error band of ±20 and ±15 % respectively.

In this study, high air velocity mist jets impinging on glass is studied, which is a first time this process is carefully studied quantitatively. The revealed first understanding will pave the road for future studies for implementations in industry. The air and water flows were controlled independently and the operational conditions included pure air flow and water mist at different liquid mass fluxes. As a result, the air and water effects are revealed independently and parametrically. The air velocity varied from 40 to 90 m/s, and the water mass flux changed from 0 to 0.145 kg/m^2 s from the multiple jets. The experiments include the effect of glass thickness on mist cooling at various air velocities and liquid mass fluxes. The duration of mist application is also investigated. The mist cooling demonstrates a definitive saving on the use of high-pressure air and the system energy requirements.

2 Spray heat transfer experiments of glass tempering

2.1 Experimental set-up

The schematic of water mist jet impingement tests is shown in Fig. 2. Before the experiments were carried out, the local flow conditions were measured at a distance of 40 mm

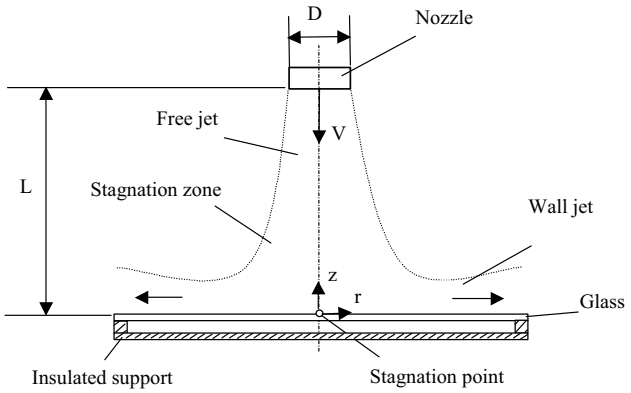

Fig. 2 Schematic of water mist jet impingement onto surface

below the nozzle. This distance affects the air velocity and droplet mass flux. The overall experimental apparatus consists of the air atomizer nozzles, an airflow system, a liquid supply system and an oven. A multiple jet nozzle setup was tested in this experiment. The multiple jet nozzle setup had seven identical nozzles installed in a triangular array. Each test had a pair of nozzle setups positioned in the opposite direction. The top view of the experimental setup schematics is shown in Fig. 3.

The test glass was vertically held by a hanger in a rail system which provides translation of the glass from the oven to the jet impingement area. Then the vertical glass was cooled from both sides with the air or mist jet impingement arrays. The jets were injected horizontally to the vertical glass sample. The heated glass was protected from the jet impingement by a removable stainless steel guard until the steady state jet impingement reached. The moment the guard was lifted, the cooling started. The distance from the exit openings of nozzles to the glass surface was 40 mm at both sides. The multiple nozzles system is shown in Fig. 4, including the air chamber and seven nozzles. It consists of an air-atomizing nozzle with a full cone spray (Nozzle # 1/8 J-SU11 from Spraying Systems Co) and an air chamber. The chamber contains three air inlets and a pressure gauge. At the exit of the air chamber, the orifice opening of the jets is 7.9 mm in diameter. The nozzles were connected with an air inlet and a water inlet. The water inlet was connected to a solenoid valve that was controlled by a timer (Newport Electronic, FTP-100 Series). The timer controls the time and the spraying time, which are manually set.

Typically, the air atomizer nozzle produced a mist of 22.7 cm^3/min (0.006 gpm) of water flow at about 22 μm volume median diameter (which was determined by Greenfield instrument at 4 cm downstream from the nozzle exit), when applied with 96.5 kPa (14 psig) air pressure and 68.9 kPa (10 psig) water pressure measured at the nozzle inlet. The total spray angle was about 13° [54].

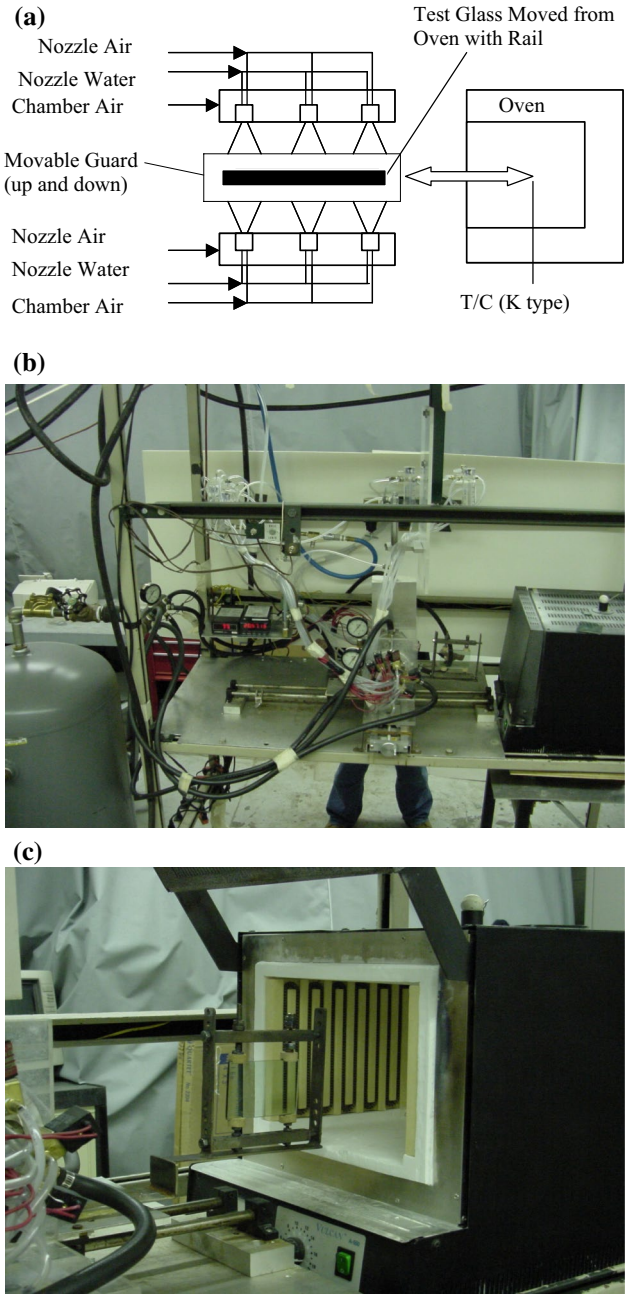

Fig. 3 **a** Experimental set-up of glass tempering (top view). **b** The experimental setup of glass tempering view. **c** The oven and rack view

The atomization air flow rate was significantly less than the chamber air flow rate. Figure 5 shows the spray image of this nozzle, which was taken by Greenfield Image Analyzer at the nozzle exit. The Greenfield (Model Speedview 700) Image Analyzer system consists of a camera with a CCD (charged coupled-device) sensor, a strobe light, interchangeable microscope lenses, digital imaging hardware and software. The spray image shows that a fine atomization was established immediately after injection with this

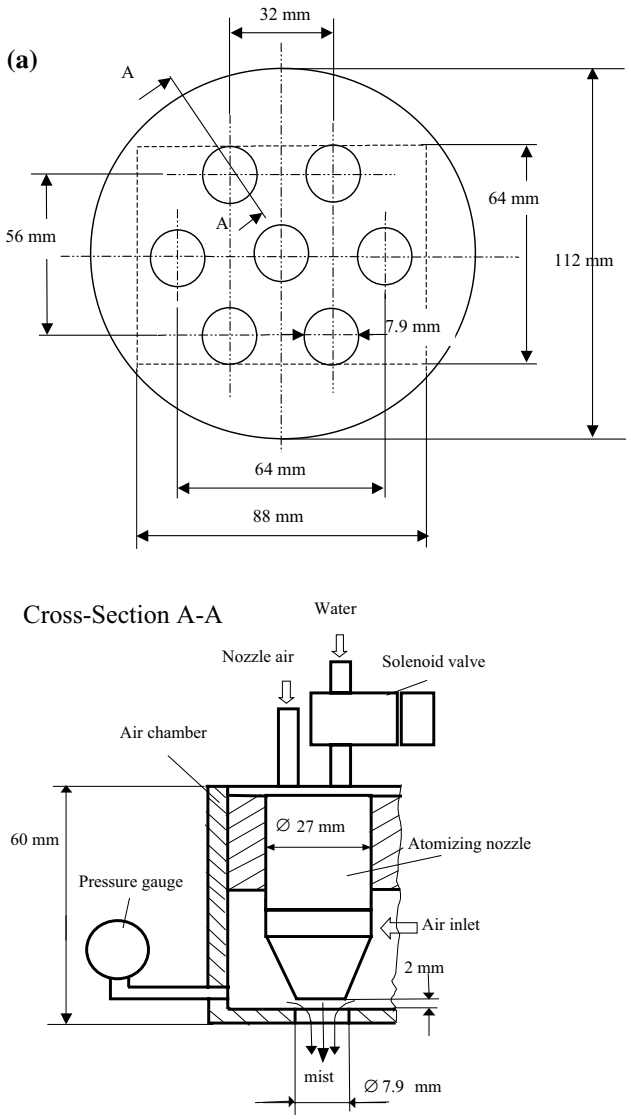

Fig. 4 **a** Plan view of multiple nozzles layout. **b** The air chambers and nozzles

Fig. 5 Spray image of the twin-fluid nozzle at 10 psig water and 14 psig atomizing air pressures

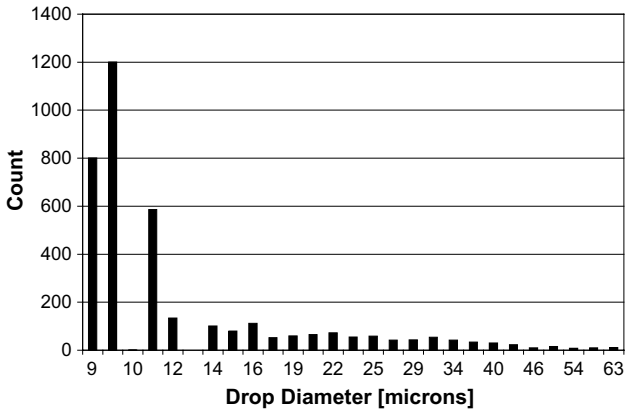

Fig. 6 Drop size distribution of the twin-fluid nozzle

twin-fluid atomizer at the given operating conditions of 14 psig air pressure and 10 psig water pressure.

Figure 6 shows the number size distribution of this spray. In air assisted water sprays, a wide range of droplets sizes can be generated during atomization based on the flow conditions of water and air flows. The typical results are shown. In this case a full conical spray type is injected from a distance of 40 mm above a stainless steel plate heated to 525 °C, and to glass plate similarly. The air and water mass flow rates are 2×10^{-3} and 10^{-4} kg/s (20:1 loading ratio), respectively. The nozzle spray angle is 13 °C and the air velocity is 35 m/s. Based on these conditions, the two phase fluid nozzle disperses a spectrum of droplet diameters ranging from 9 to 63 μm with an average diameter of 19.2 μm by volume.

Two different sizes of glass samples were tested with air and mist cooling. The first (small) glass sample has

dimensions 2.5 cm by 2.5 cm (1 inch by 1 inch) and the second (large) one has dimensions 6.35 cm by 8.89 cm (2.5 inch by 3.5 inch). The small samples were only used for preliminary tests, and the results of larger samples are reported in this paper. For both types of glass samples, the glass thicknesses were 2.1, 2.85, 3.2, and 4 mm. Each nozzle covers an area of 8.64 cm^2 considering the arrangement is in a form of an infinite array. This value is used to evaluate the equivalent water volume flux. The vertical hanging structure of the glass plate is made of stainless steel and fits well into the oven. There are two clips to hang the glass at high temperatures.

The total water flow rate is varied from 0 to 14 cm^3/min for the multiple nozzles. The air chamber pressure provides between 40 and 90 m/s air jet velocity for multiple nozzles. The air chamber pressure versus the mist velocity is calibrated. All the experiments are conducted under a well-controlled procedure. The oven was uniformly pre-heated to 740 °C (1350 °F) and the temperature was measured by a thermocouple installed inside the oven and monitored by the digital temperature meter. The glass was then slid into the oven and heated inside the oven for 5 min. The guard shuttle was set at the test location to block the mist flows, and the spraying time was set manually. The resolution of the spraying time setting was 0.01 s. After the glass was heated uniformly, the sliding rail as shown in Fig. 3c was slid out to the spraying position in the guard shutter. The shutter was opened, and water mist was injected onto the heated surface for the programmed time duration. Afterwards, the water flow was terminated, but the air injection was continued for further cooling of the glass surfaces. After the cooling process, the glass sample was tested for the extent of tempering. For the small glass samples of single nozzles, the puncturing tip was pinched onto the center of the tempered glass with a spring force. For the larger samples of multiple nozzles, the puncturing tip was pinched onto the corner of the tempered glass. According to the pattern and counting of broken fragments, the quality of tempered glass was revealed and compared. For the large samples, the counting was made over an area of 3.81 cm by 3.81 cm (1.5 inch by 1.5 inch).

During the tempering of glass using a water mist, the effective cooling must occur when the glass is above the annealing temperature. The water mist should be terminated when the glass falls below the Leidenfrost temperature. Also, it is important to make sure that the cooling front penetrates into the glass as much as possible. If the surface-cooling rate due to water mist is very high, the total duration of the cooling will be short because the surface temperature drops below the Leidenfrost temperature quickly. But a short mist cooling duration will not be able to let the cooling front penetrate enough into the glass. Conversely, if the surface-cooling rate due to water mist is too small, the total duration of cooling will be long, and penetration of the cooling front into the glass will be sufficient. However, the small cooling rate will produce a small temperature gradient in the glass, and the resulting tempering will be insufficient. As a result, for a given air jet flow rate, an optimal condition of the water mass flux and duration of water mist application shall exist. This optimal condition will also depend upon the thickness of the glass.

There are several factors that may cause the glass to break during or right after the water mist application. The impingement forces or the deposition pattern caused by the mist during the cooling process may not be even on the glass surface, and it can cause cracks during the mist cooling process. If the applied amount of water mist is too high, the glass will crack instantly due to the severe transient thermal stress building up inside the glass at the first moment of mist contacts. The glass cracks if the glass surface temperature falls below the Leidenfrost temperature but the water mist is continued. As result, it is desirable to have a relatively low mass flux of mist applied for a reasonably long time. In general, the higher the mass flux, the shorter will be the time of mist application.

2.2 Experimental uncertainty

In the glass tempering process an Infrared Pyrometer was used to measure the glass surface temperature. The Pyrometer was calibrated by a K-type thermocouple. The emissivity of 0.81 was selected after the calibration.

The thickness of glass plate is ranged from 2.1 to 4 mm and the temperature difference between front side and backside during cooling is estimated to be within couple degrees. The cooling data, taken between 525 and 500 °C, are used to evaluate the change in temperature with time, dT/dt. Since this is well within the film-boiling regime, the rate of change in temperature is steady. Therefore, all the consistent errors, such as the assumption of lumped approach, will not much affect dT/dt and the results of data reduction. This also reduces the possible error because the inversed conduction is not used. The estimated error of the deduced heat transfer coefficient is therefore in the order of 0.4 % mainly due to the uncertainty of thermocouples readings. The radiation heat loss was included in the heat transfer evaluation for mist cooling. A possible source of error comes from the calibration of surface emissivity during the pure air-cooling tests. Considering a 5 % error of the natural convection formula, the resulting error on the estimated emissivity will be order of 7 %. When this emissivity is used, an estimated error on heat transfer coefficient will be order of 0.86 %. The measurement error of the air velocity is within 0.1 % which is about 0.1 m/s. The water mass flux is within 1 % which is about 0.00145 kg/m^2s. Combining these data reduction uncertainties including the

contributions of thermocouple reading, the emissivity estimation, the air velocity and water mass flux measurements, the overall uncertainty of heat transfer coefficient is 1.4 % [4, 55].

3 Results and discussion

The fundamental mechanism of mist cooling is revealed from the experiments of a single water mist jet impinging on hot stainless steel plates [4]. Since the droplet are small, heat transfer distributions and improvement of water mist has a similar form as the enhanced air jet cooling. A major finding is that the heat transfer contributions of air and of mist are separable, and the results are additive to make the total heat transfer.

During the tempering of glass with water mist, effective cooling occurs when the glass temperature is above the glass annealing temperature. On the other hand, water mist should be terminated when the glass temperature falls below its Leidenfrost temperature. Also, it is desirable to make the cooling front penetrates into the glass as much as possible. If the surface cooling rate due to water mist is very high, the total duration of cooling must be short because the surface temperature drops below the Leidenfrost temperature quickly. However, the short mist cooling duration will not be able to let the cooling front penetrate sufficiently into the glass. Conversely, if the surface cooling rate due to water mist is too small the total duration of cooling will be long, and penetration of the cooling front into the glass will be sufficient. However, the small cooling rate will produce a small temperature gradient in the glass, and the resulting tempering will be insufficient. As a result, for a given air jet flow rate, an optimal condition of the water mass flux and duration of water mist application shall exist. This optimal condition will also depend on the thickness of the glass.

In practice it has been difficult to use mist cooling for tempering. There are several factors that may cause the glass to break during or right after the water mist application. Some of the factors can be described as follows:

1. The impingement forces or the deposition pattern caused by the mist during the cooling process may be uneven on the glass surface, and this can cause uneven stress, which leads to cracks during the mist cooling process.
2. The application of the amount of water mist is too high, and the glass will crack instantly when the mist is initially applied due to the severe transient thermal stress building up in the glass at the instant water mist makes first contact.
3. When the glass surface temperature falls below the Leidenfrost temperature, the glass surface cracks if water mist spraying continues. Generally, the higher the mass flux, the shorter will be the time of mist application to avoid mist cooling below the Leidenfrost temperature.
4. As result, it is desirable to have an optimal mass flux of mist application that it is high enough to induce sufficient tempering of glass but low enough to give a reasonably long time of cooling.

3.1 Glass test experiments

A side view of glass tempering process from both sides with multi-spray mist injections (7 nozzles on each side) is shown in Fig. 7. The vertically placed glass can be seen in the middle of this image, where both surfaces were cooled down by horizontally injected mist spray. Various experimental conditions are studied. The air velocity is varied from 40 to 90 m/s. A point force is applied at the lower left corner of glass plate (0.5 inch by 0.5 inch from sides) to fracture the glass after the tempering process in order to quantify the quality of the tempering process. The fracture particles count of the tempered glass within an area of 14.5 cm^2 (2.25 $inch^2$) versus water flow rate per nozzle (or mass flux) is plotted for different operating conditions.

A typical comparison of fracturing count on the tempered glass is shown in Fig. 8. The number of fractured particles per unit area is generally an indication of the residual stress buildup in the glass after the tempering process. The higher this stress the smaller the particles. The results of a tempering process of 46.8 m/s air velocity on 3.2 mm glass thickness with pure air-cooling and with 2 cm^3/min water mist cooling are displayed. The particles count is

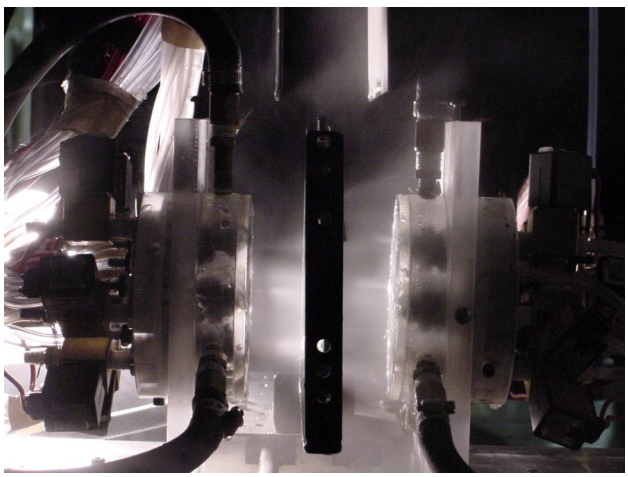

Fig. 7 Glass tempering from both sides with multi-spray mist injections (7 nozzles in each side)

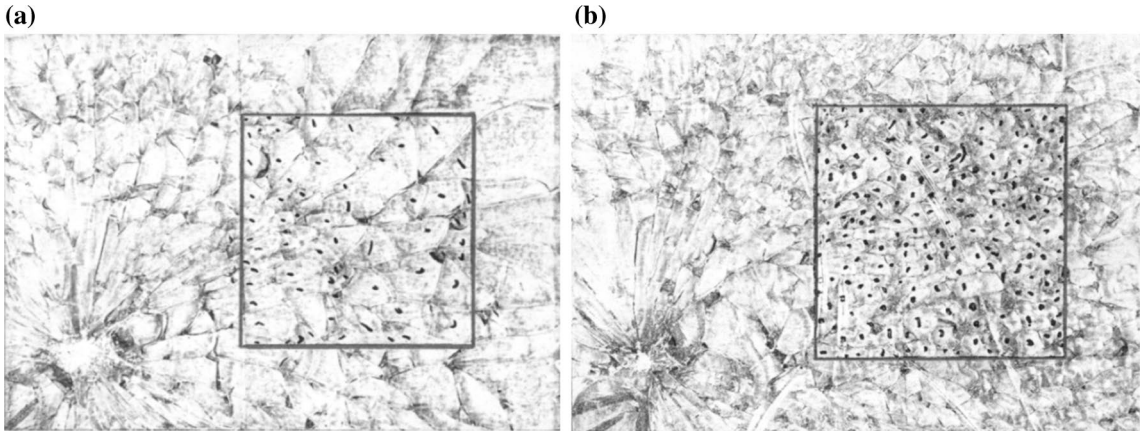

Fig. 8 A typical comparison of fracturing count on the tempered glass 3.2 mm (46.8 m/s air velocity). **a** Pure air-cooling. **b** Water mist cooling (2 cm^3/min water mist)

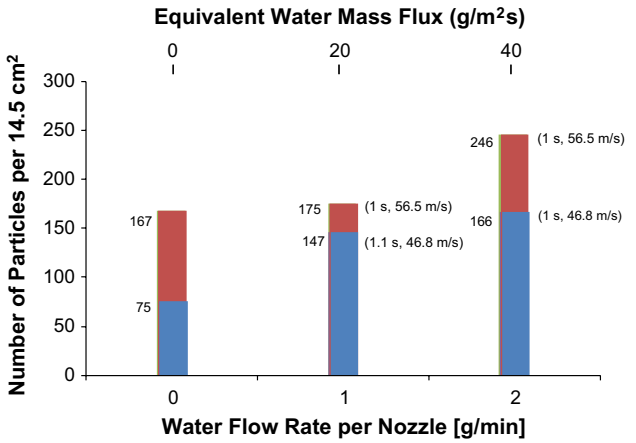

Fig. 9 A comparison of particles count on 3.2 mm glass thickness at 46.8 and 56.5 m/s air velocity

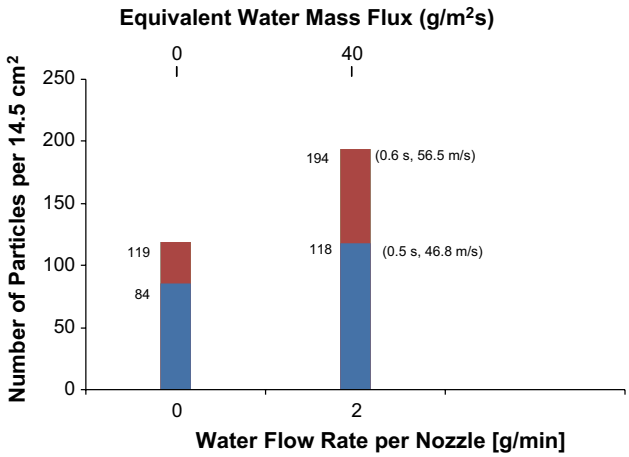

Fig. 10 A comparison of particles count on 2.85 mm glass thickness at 46.8 and 56.5 m/s air velocity

conducted on a small area of 14.5 cm^2. The improvement of fracturing count due to water mist is shown.

The trend of the results is shown for medium air velocity at various mist flow rates and different glass thicknesses. Two test cases for a glass thickness of 3.2 mm and air velocity of 46.8 and 56.5 m/s are compared.

Figure 9 shows the number of particles per 14.5 cm^2 (2.25 $inch^2$) as a function of the water flow rate per nozzle at an air velocity of 46.8 and 56.5 m/s for the 3.2 mm auto glass. The average number of counted particles are 75 for 46.8 m/s and 167 for 56.5 m/s when pure air-cooling. This increases to 166 particles for the 46.8 m/s air velocity and 246 particles for the 56.5 m/s air velocity when air mist sprayed for 1 s at a water flow rate of 2 cm^3/min (with 1 s being the maximum spraying time). Beyond this time limit the glass will crack in both mist cooling cases. The same safety limit is also given for other glass cases in

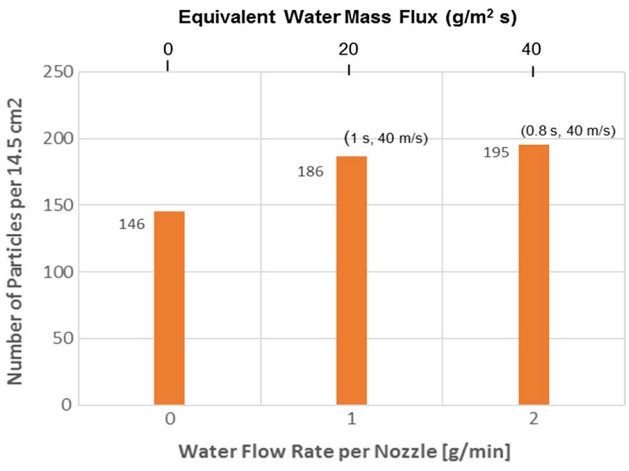

Fig. 11 A comparison of particle counts on 4 mm glass thickness at 40 m/s air velocity

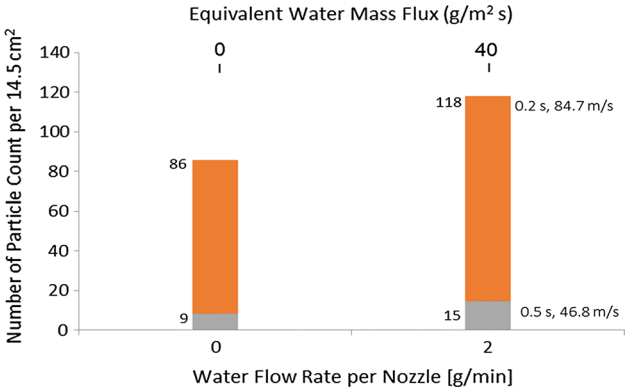

Fig. 12 A comparison of particles count on 2.1 mm glass at 46.8 and 84.7 m/s air velocity

Figs. 10, 11 and 12. The number of particles is increased by 121 % for the air velocity of 46.8 m/s and by 47 % for the air velocity of 56.5 m/s when cooling by water mist. It has been observed that the heat transfer contributions of air and water are additive in the mist cooling [3–5]. From this test, the presence of water mist increases the overall cooling and induces substantial residual stress in the glass and achieves better tempering. The longer the time of the mist application is, the better are the results.

Figure 10 shows the effect of water mist cooling for an air velocity of 46.8 and 56.5 m/s on 2.85 mm thick auto glass. For pure air cooling with an air velocity of 46.8 and 56.5 m/s, the average number of particles are 84 and 119 respectively. For the 46.8 m/s air velocity, the number of particles increases to 118 when water mist is sprayed for 0.5 s at a flow rate of 2 cm^3/min. The number of particles is shown to increase by 29 %. For the air velocity of 56.5 m/s, the average number of particles is shown to increase from 119 particles when pure air-cooling is used to 194 particles when water mist is sprayed for 0.6 s at water flow rate of 2 cm^3/min. The number of particles is shown to increase by 63 %.

Figure 11 shows a comparison in the number of particles per 14.5 cm^2 as a function of the water flow rate per nozzle (or equivalent water flux) for an air velocity of 40 m/s on a 4 mm thick glass. The average number of particles is 146 when pure air-cooling is used, but is 195 when water mist is sprayed for 0.8 s at a water flow rate of 2 cm^3/min. The number of particles is increased by 34 % for the water mist cooling.

A comparison in the number of particles at an air velocity of 46.8 and 84.7 m/s for the 2.1 mm auto glass is shown in Fig. 12. The average number of particles is 9 for the pure air-cooling, but is 15 for the water mist cooling at a water flow rate of 2 cm^3/min for a spraying period of 0.5 s. The number of particles is increased by 71 % when cooling by water mist. Consistently, mist enhances the tempering process such that the fracturing results are improved with higher mass flux. In most cases, the time duration of the spray application is reasonably manageable (more than half a second). For the very thin glass of 2.1 mm, it is generally understood that air-cooling does not temper the glass easily. As shown in Fig. 12, pure air-cooling gives only 9 fracturing counts. However, when using water mist, the count increases to 15, which is a significant improvement. However, this is still not very acceptable from a safety standard viewpoint.

In order to get a large count or the tempering stress for 2.1 mm thick glass, the experiment is done at a high air velocity of 84.7 m/s. Figure 12 also shows typical fracturing results as a function of the water flow rate per nozzle at an air velocity of 84.7 m/s for the 2.1 mm thick auto glass. Pure air-cooling gives an average fracturing count of 86. The addition of water mist brings the average count up to 118. The number of particles is increased by 38 % for the water mist cooling. However, the maximum tolerable time duration of the mist cooling application is 0.2 s, which is feasible in the laboratory but difficult in practice.

When the tempered glass is made by mist cooling without fracture, air pressure is reduced significantly. This reduction is about 29 % air pressure reduction for 2-mm glass plate and 50 % reduction for both 3- and 4-mm glass. When water mist is added, air pressure is reduced and the same particle counts are obtained in the original air cooling and the mist cooling at reduced pressure. The saving of the air pumping power is validated. For the 2.1 mm thick glass plate almost same number of particle counts obtained at 84.7 m/s air velocity of pure air cooling is observed at 56.5 m/s air velocity with 2 cc/min (0.4 s) mist cooling. Also, when the glass thickness was 3 mm, almost the same number of particles count obtained at 73 m/s air velocity of pure air cooling is observed at an air velocity of 46.8 m/s with 2 cc/min (0.8 s) mist cooling. Similarly, the same observation applies to the 4 mm thick glass plate with 84.7 m/s pure air cooling and 56.5 m/s with 1 cc/min (0.4 s) mist cooling.

From these experiments the time limit of the duration of mist application is dependent upon the glass thickness. For example, the maximum durations of mist applications are 0.2 s for 2 mm glass, 0.5 s for 2.8 mm, 1 s for 3.2 mm, and 0.8 s for 4 mm glass. In general, the thicker the glass, the longer is the time spray mist can be applied. This is due to the thick glass has a higher energy content in the glass and the slower cooling to the Leidenfrost temperature on its surface.

It is desirable to explore the effectiveness of mist cooling at low air velocity due to the potential saving on compressed air supply. It is generally observed that the addition of water mist significantly improves the fracturing results. The longer the time of the mist application is, the better are the results.

4 Conclusions

Spray cooling experiments were conducted to reveal the heat transfer enhancement of dilute water mist on high temperature glass surfaces. Based upon the previous studies of the authors [3–5, 41, 42], the basic understanding is obtained. With a small amount of water in the air jet, the heat transfer is dramatically increased. The water mist heat transfer coefficient increases with both the air velocity and the liquid mass flux. Mist and air heat transfer are rather independent. Mist heat transfer increases almost linear with the water mass flux. The velocity effect is relatively small. The overall convective heat transfer coefficient can be viewed as two separable elements, which is the summation of the heat transfer coefficients of air and of liquid mass flux, respectively. Due to the fine droplets, the normalized radial distribution of mist flow heat transfer is similar to that of pure air jets. The Leidenfrost temperature increases with both the air velocity and the liquid mass flux.

Pure air cooling has been investigated in glass tempering process. The high air velocity jet impingement has been applied during the cooling process of glass tempering. In the conventional process of glass tempering by air-jets, the air velocity is about 100 m/s. Also the increase in the air jet velocity produces an undesirable deformation in the glass plate. In addition, the high velocity increases the electricity cost for air compression; therefore, an efficient alternative high cooling method for a thin glass plate tempering is required.

Water mist can be used to reduce the extensive use of high-pressure air for tempering of glass. In this study, high air velocity mist jets impinging on glass is studied, which is a first time this process is carefully studied quantitatively. The revealed first understanding will pave the road for future studies for implementations in industry.

For multiple nozzle tests on glass with thicknesses of more than 3 mm, the residual stress as represented in the particle counts after fracturing due to the presence of water mist, which improves from the pure-air jets by about 121 %. For 2 mm glass, it is found that the air velocity should be much higher to reach the desirable range of the residual stress. At this condition, the air mist gives an improvement of about 38 % over the pure air cooling. However, the duration of the water mist application should be short (as short as 0.2 s in the cases of thin glass) to avoid the fracturing of the glass due to the rapid cooling toward the Leidenfrost temperature. This is because when water mist is applied to a surface after the surface temperature is cooled below the Leidenfrost temperature, local nucleate boiling occurs. The heat flux rate of nucleate boiling is very high. Therefore, slight uneven thermal stress distribution could induce cracks of the glass. Furthermore, it is possible to find the optimal water flux and duration of mist application to achieve a desirable temperature distribution in the glass for deep penetration of the cooling front and large residual stress of tempering but without inducing cracking during the tempering.

Mist spray cooling process has a high heat transfer, which could allow for the reduction of compressed air used in tempering. The test results indicate that thin and low-cost tempered glass can be made by mist cooling without fracture and with about 29 % air pressure reduction for 2-mm glass plate and 50 % reduction for both 3- and 4-mm glass plates.

Acknowledgments The financial support of Libbey-Owens-Ford Co. (now Pilkington) during the study is greatly appreciated.

References

1. Issa RJ (2009) Multiphase spray cooling technology in industry. In: Jayanthakumaran K (ed) Advanced technologies. InTech, ISBN: 978-953-307-009-4
2. Mishra PC, Nayak SK, Pradhan P, Ghosh DP (2015) Impingement cooling of hot metal strips in runout table—a review. Interfacial Phenom Heat Transf 3(2):117–137
3. Sozbir N, Yao SC (2002) Investigation of water mist cooling for glass tempering. In: ASME international 6th biennial conference on engineering systems design and analysis (ESDA), Istanbul, Turkey, 8–11 July 2002
4. Sozbir N, Chang YW, Yao SC (2003) Heat transfer of impacting water mist on high temperature metal surfaces. J Heat Transf 125:70–74
5. Sozbir N, Chang YW, Yao SC (2004) Experimental investigation of water mist cooling for glass tempering. At Sprays 14(3):191–210
6. Handy Manual Glass Industry, Output of a seminar on energy conservation in glass industry (1993) UNIDO and Ministry of Industrial Development and Industry (MITI), Organized by the energy conservation center (ECC), Japan
7. Worrell E, Galitsky C, Masanet E, Graus W (2008) Energy efficiency improvement and cost saving opportunities for the glass industry. Report, Lawrence Berkeley National Laboratory
8. Gardon R (1961) A review of radiant heat transfer in glass. J Am Ceram Soc 44:305–312
9. Gardon R (1980) Thermal tempering of glass. In: Uhlmann DR et al (eds) Glass science and technology, vol 5. Academic Press, New York, pp 145–216
10. Garciamoreno CJ, Atreya A, Everest DA (2003) Heat transfer in glass quenching. Energy and high performance facility sourcebook. In: Garciamoreno CJ et al (eds), pp 299–350
11. Garciamoreno CJ, Everest DA, Atreya A (2015) Heat transfer in glass quenching for glass tempering, In: 75th Conference on Glass Problems (GPC), Columbus, OH, pp 235–252
12. Lee KH, Viskanta R (1988) Quenching of flat glass by impinging air jets. Numer Heat Transf Part A 33(1):5–22
13. Ohkubo H, Nishio S (1988) Mist cooling for thermal tempering of glass. Jpn Soc Mech Eng Int J Ser II 31(3):444–450
14. Ping TH, Lallemand M (1989) Transient radiative-conductive heat transfer in flat glasses submitted to temperature, flux and mixed boundary, conditions. Int J Heat Mass Transf 32:795–810
15. Field RE, Viskanta R (1990) Measurement and prediction of the temperature distribution in soda-lime glass plates. J Am Ceram Soc 73:2047–2053

16. Su MH, Sutton WH (1995) Transient conductive and radiative heat transfer in a silica window. J Thermophys Heat Transf 9:370–373
17. Kormanyos KR (1997) Controlled differential forced convection heating for glass tempering processs. J Non Cryst Solids 218:235–241
18. Monnoyer F, Lochegnies D (2008) Heat transfer and flow characteristics of the cooling system of an industrial glass tempering unit. Appl Therm Eng 28:2167–2177
19. Lochegnies D, Monnoyer F (2009) A 3D computation method for evaluating the impact of heat transfer on residual stress in thermal tempering of flat glass. Glass Technol Eur J Glass Sci Technol Part A 50:6
20. Makarov RI, Suvorov EV (2010) Increasing the quality of tempered glass on an operating processs line. Glass Ceram 67(5–6):138–141
21. Nielsen JH, Olesen JF, Poulsen PN, Stang H (2010) Finite element implementation of glass tempering model in three dimensions. Comput Struct 88:963–972
22. Golcu M, Yazıcı H, Akçay M (2012) Experimental Investigation of cooling with multiple air jets on auto glass tempering. J Fac Eng Archit Gazi Univ 27(4):775–783
23. Yazıcı H, Akçay M, Golcu M, Koseoglu MF, Sekmen Y (2012) Experimental investigation of the transient cooling characterictics of an industrial glass tempering unit. World Acad Sci Eng Technol 61:207–211
24. Akçay M, Sekman Y, Golcu M (2014) The effect of heating and cooling temperatures on rapid cooling time and particle number in auto glass tempering process. J Fac Eng Archit Gazi Univ 29(3):605–615
25. Yazıcı H, Akçay M, Golcu M, Koseoglu MF, Sekmen Y (2015) Experimental investigation of the transient temperature distribution and heat transfer by jet impingement in glass tempering process. IJST Trans Mech Eng 39(M2):337–349
26. Akçay M, Yazıcı H, Golcu M, Sekmen Y (2016) The effect of different cooling unit configurations and cooling temperature on glass tempering quality. At Sprays 26(10):1051–1067
27. Nacheva M, Schmidt J (2008) Micro model for the analysis of spray cooling heat transfer-influence of droplet parameters, micro-macro-interaction. In: Bertram A, Tomas J (eds) Micro-macro-interactions in structured media and particle systems. Springer, Berlin, pp 159–172
28. Deb D, Yao SC (1989) Analysis on film boiling heat transfer of impacting sprays. Int J Heat Mass Transf 32:2099–2112
29. Graham KM, Ramadhyani S (1996) Experimental and theoretical studies of mist jet impingement cooling. ASME. J Heat Transf 118:343–349
30. Cox TL, Yao SC (1999) Heat transfer of sprays of large water drops impacting on high temperature surfaces. J Heat Transf Trans ASME 121(2):446–450
31. Yao SC, Cox TL (2002) A general heat transfer correlation for impacting for water sprays on high temperature surfaces. Exp Heat Transf 5(4):207–219
32. Issa RJ, Yao SC (2005) Numerical model for spray-wall impaction and heat transfer at atmospheric conditions. J Thermophys Heat Transf 19(4):441–447
33. Issa RJ, Yao SC (2005) A numerical model for the mist dynamics and heat transfer at various pressures. J Fluids Eng Trans ASME 127(4):631–639
34. Moreira ALN, Carvalho J, Panao MRO (2007) An experimental methodology to quantify the spray cooling event at intermittent spray impact. Int J Heat Fluid Flow 28:191–202
35. Al-Ahmedi H, Yao SC (2008) Spray cooling of high metals using high mass flux industrial nozzles. Exp Heat Transf 21(1):38–54
36. Hernandez IC, Acosta FG, Castillejos AHE, Minchaca JIM (2008) The Fluid dynamics of secondary cooling air-mist jets. Metall Mater Trans B 39B:746–763
37. Lyons OFP et al (2009) Time averaged and fluctuating heat transfer measurements in an atomizing mist jet nozzle. In: ASME International Mechanical Engineering Congress and Exposition, 13–19 November 2009, Lake Buena Vista, Florida, USA
38. Panao MRO and Moreira ALN (2009) Heat transfer correlation for intermittent spray impingement: a dynamic approach. Int J Therm Sci 48:1853–1862
39. Santangelo PE (2010) Characterization of high-pressure water-mist sprays: experimental analysis of droplet size and dispersion. Exp Therm Fluid Sci 34:1353–1366
40. Cheng W, Liu Q, Zhao R et al (2010) Experimental investigation of parameters effect on heat transfer of spray cooling. Heat Mass Transf 46(8):911–921
41. Zhao R, Cheng W, Liu Q, Fan H (2012) Study on heat transfer performance of spray cooling: model and analysis. Heat Mass Transf 46:821–829
42. Sozbir N et al (2010) Multiphase spray cooling of steel plates near the ledenfrost temperature-experimental studies and numerical modeling. At Sprays 20(5):387–405
43. Yiğit C, Sozbir N, Yao SC, Güven HR, Issa RJ (2011) Experimental measurements and computational modeling for the spray cooling of a steel plate near the leidenfrost temperature. J Therm Sci Technol 31(1):27–36
44. Panao MRO, Moreira ALN, Durao DFG (2011) Thermal-fluid assessment of multi jet atomization for spray cooling applications. Energy 36:2302–2311
45. Panao MRO, Correia AM, Moreira ALN (2012) High-power electronics thermal management with intermitted multi jet sprays. Appl Therm Eng 37:293–301
46. Lyons OFP et al (2012) Heat transfer and flow in an atomizating mist jet: a combined hot film and shadowgraph imaging approach. In: 6th European thermal sciences conference (Eurotherm 2012), Journal of Physics: Conference Series, vol 395. doi:10.1088/1742-6596/395/1/012173
47. Bellerová H, Tseng AA, Pohanka M et al (2012) Heat transfer of spray cooling using alumina/water nanofluids with full cone nozzles. Heat Mass Transf 48:1971. doi:10.1007/s00231-012-1037-3
48. Yan ZB, Duan F, Wong TN et al (2013) Large area impingement spray cooling from multiple normal and inclined spray nozzles. Heat Mass Transf 49(7):985–990
49. Ravikumar SV, Jha JM, Mohapatra SS et al (2013) Experimental study of the effect of spray inclination on ultrafast cooling of a hot steel plate. Heat Mass Transf 49(10):1509–1522
50. Mohapatra SS, Ravikumar SV, Jha JM et al (2014) Ultra fast cooling of hot steel plate by air atomized spray with salt solution. Heat Mass Transf 50(5):587–601
51. Panao MRO, Delgado JMF (2014) Toward the design of low flow-rate multi jet impingement spray atomizers. Exp Therm Fluid Sci 58:170–179
52. Aamir M, Liao Q, Hong W et al (2016) Transient heat transfer behavior of water spray evaporative cooling on a stainless steel cylinder with structured surface for safety design application in high temperature scenario. Heat Mass Transf. doi:10.1007/s00231-016-1830-5
53. Agrawal C, Kumar R, Gupta A et al (2016) Rewetting of hot vertical rod during jet impingement surface cooling. Heat Mass Transf 52(6):1203–1217
54. Industrial Spray Products, Spraying Systems Co. Catalog 60, Wheaton, IL
55. Holman JP (2001) Experimental methods for engineers, 7th edn. McGraw-Hill, NY